

A ^2H NMR Relaxation Experiment for the Measurement of the Time Scale of Methyl Side-Chain Dynamics in Large Proteins

Vitali Tugarinov* and Lewis E. Kay*

Contribution from the Departments of Medical Genetics, Biochemistry, and Chemistry,
University of Toronto, Toronto, Ontario, Canada M5S 1A8

Received May 2, 2006; Revised Manuscript Received July 19, 2006; E-mail: kay@pound.med.utoronto.ca; vitali@pound.med.utoronto.ca

Abstract: An NMR experiment is presented for the measurement of the time scale of methyl side-chain dynamics in proteins that are labeled with methyl groups of the $^{13}\text{CHD}_2$ variety. The measurement is accomplished by selecting a magnetization mode that to excellent approximation relaxes in a single-exponential manner with a T_1 -like rate. The combination of $R_1(^{13}\text{CHD}_2)$ and $R_2(^{13}\text{CHD}_2)$ ^2H relaxation rates facilitates the extraction of motional parameters from $^{13}\text{CHD}_2$ -labeled proteins exclusively. The utility of the methodology is demonstrated with applications to proteins with tumbling times ranging from 2 ns (protein L, 7.5 kDa, 45 °C) to 54 ns (malate synthase G, 82 kDa, 37 °C); dynamics parameters are shown to be in excellent agreement with those obtained in ^2H NMR studies of other methyl isotopomers. A consistency relationship is found to exist between $R_1(^{13}\text{CHD}_2)$ and the relaxation rates of pure longitudinal and quadrupolar order modes in $^{13}\text{CH}_2\text{D}$ -labeled methyl groups, and experimental rates measured for a number of proteins are shown to be in excellent agreement with expectations based on theory. The present methodology extends the applicability of ^2H relaxation methods for the quantification of side-chain dynamics in high molecular weight proteins.

Introduction

Deuterium NMR line-shape and spin relaxation experiments have long provided important insights into molecular dynamics.^{1–3} Although the earliest applications of the methodology to biological systems date back some 30 years now, studies of protein dynamics using ^2H relaxation and high resolution solution NMR spectroscopy have only emerged in the past decade. Techniques are now available for the quantification of side-chain mobility in both small^{4,5} and large⁶ protein molecules, with most of the developments centered on either $^{13}\text{CH}_2\text{D}$ methyl^{4,5} or ^{13}CHD methylene⁷ probes. Recently, our laboratory has shown that transverse relaxation rates can also be measured in $^{13}\text{CHD}_2$ -labeled methyl groups of large proteins and that from such rates, $R_2(^2\text{H}, ^{13}\text{CHD}_2)$, accurate order parameters (S_{axis}) characterizing the amplitude of methyl axis motions can be extracted.⁶ Applications to malate synthase G (MSG),⁸ a 723-residue enzyme, have established the utility of the methodology.⁹ In some respects, $^{13}\text{CHD}_2$ moieties offer advantages over $^{13}\text{CH}_2\text{D}$ groups in studies involving large proteins because (i) $^{13}\text{CHD}_2$ -directed ^2H transverse relaxation experiments are more

sensitive in comparison with experiments that focus on $^{13}\text{CH}_2\text{D}$ groups, although at the cost of somewhat reduced resolution,⁶ and (ii) an independent verification of extracted S_{axis} values can be obtained through sensitive ^{13}C relaxation measurements recorded on the same sample.^{9,10} It is also noteworthy that the recently developed stereoarray isotope labeling (SAIL) technology for side chains¹¹ produces proteins with methyl groups of the $^{13}\text{CHD}_2$ variety, so that structural and dynamics studies can be performed on identical samples.

Despite the promise of using the deuterons in the $^{13}\text{CHD}_2$ moiety as probes of methyl dynamics, one drawback that emerges with this type of labeling at present is the lack of an experiment that measures longitudinal ^2H relaxation rates, from which the time scale of the motions of the methyl side chain can be obtained. As discussed previously, in studies of large proteins $R_2(^2\text{H}, ^{13}\text{CHD}_2)$ rates are directly proportional to the amplitude of motion but provide essentially no information about the time scale of internal dynamics. Here we describe a new pulse scheme that measures the relaxation of a magnetization mode, M_L , that is carefully created from a linear combination of ^{13}C lines in the $^{13}\text{CHD}_2$ methyl group, separated in frequency by the one-bond ^{13}C – ^2H scalar coupling, J_{CD} . We show that this magnetization mode relaxes in a near single-exponential fashion and that it reports directly on the time scale of motion. The methodology is demonstrated on a number of protein systems with rotational correlation times ranging from 2 to 54 ns, and the results obtained are shown to be consistent with

- (1) Seelig, J. *Q. Rev. Biophys.* **1977**, *10*, 353.
- (2) Jelinski, L. W.; Sullivan, C. E.; Torchia, D. A. *Nature* **1980**, *284*, 531.
- (3) Vold, R. R.; Vold, R. L. *Adv. Magn. Reson.* **1991**, *16*, 85.
- (4) Muhandiram, D. R.; Yamazaki, T.; Sykes, B. D.; Kay, L. E. *J. Am. Chem. Soc.* **1995**, *117*, 11536–11544.
- (5) Millet, O.; Muhandiram, D. R.; Skrynnikov, N. R.; Kay, L. E. *J. Am. Chem. Soc.* **2002**, *124*, 6439–6448.
- (6) Tugarinov, V.; Ollerenshaw, J. E.; Kay, L. E. *J. Am. Chem. Soc.* **2005**, *127*, 8214–8225.
- (7) Yang, D.; Mittermaier, A.; Mok, Y. K.; Kay, L. E. *J. Mol. Biol.* **1998**, *276*, 939–954.
- (8) Howard, B. R.; Endrizzi, J. A.; Remington, S. J. *Biochemistry* **2000**, *39*, 3156–3168.
- (9) Tugarinov, V.; Kay, L. E. *Biochemistry* **2005**, *44*, 15970–15977.

- (10) Ishima, R.; Petkova, A. P.; Louis, J. M.; Torchia, D. A. *J. Am. Chem. Soc.* **2001**, *123*, 6164–6171.
- (11) Kainosho, M.; Torizawa, T.; Iwashita, Y.; Terauchi, T.; Mei Ono, A.; Guntert, P. *Nature* **2006**, *440*, 52–57.

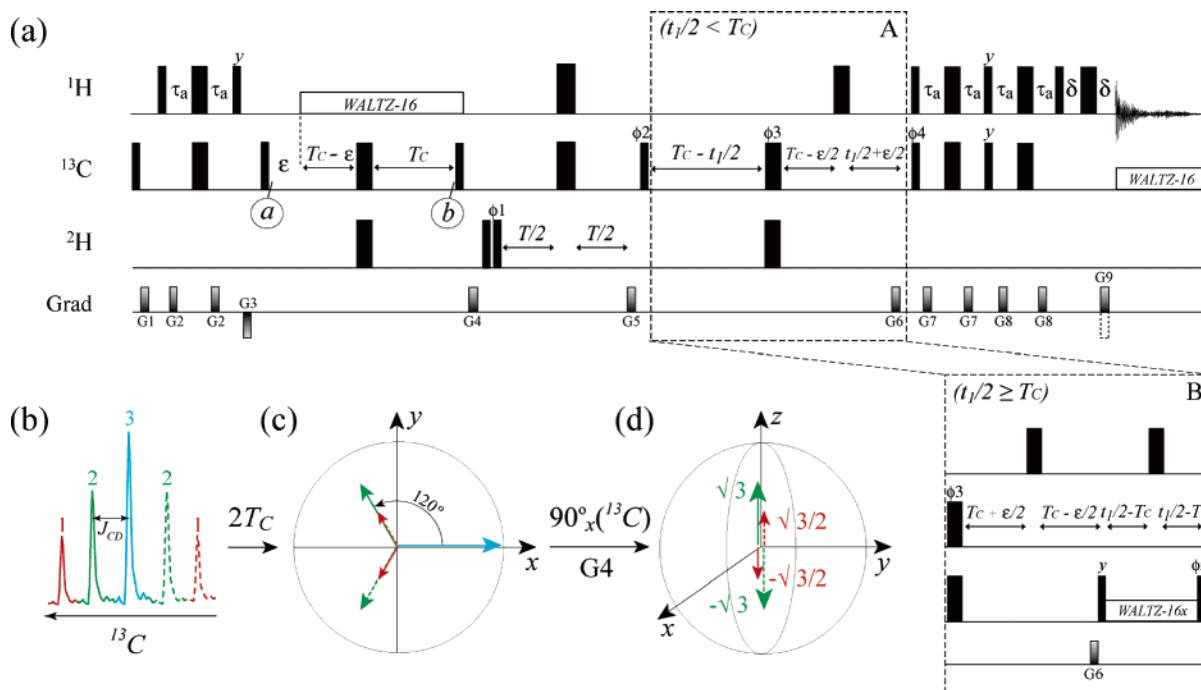


Figure 1. (a) Pulse scheme for the measurement of ^2H T_1 -like relaxation of the magnetization mode M_L in $\{\text{U-}[^{12}\text{C},^2\text{H}]; \text{methyl-}^{13}\text{CHD}_2\}$ -labeled proteins for (A) $t_1/2 < T_C$ and (B) $t_1/2 \geq T_C$. All narrow (wide) rectangular pulses are applied with flip angles of 90° (180°) along the x -axis unless indicated otherwise. All ^1H and ^{13}C pulses are applied with the highest possible power, while a 2 kHz field is used for ^2H pulses. ^{13}C and ^1H WALTZ-16 decoupling²⁰ elements use 1.2 and 5.6 kHz fields, respectively, while ^2H decoupling is achieved with a 0.7 kHz field. Delays are as follows: $\tau_a = 1.8$ ms; $\epsilon = 4.0$ ms; $\delta = 0.35$ ms; $T_C = 8.7$ ms; T is a variable relaxation delay. The durations and strengths in units of (ms;G/cm) are as follows: G1 = (1;7.5); G2 = (0.5;10); G3 = (1;-8); G4 = (0.5;6); G5 = (0.5;18); G6 = (0.5;30); G7 = (0.3;2.5); G8 = (0.3;7); G9 = (0.125;-29.5). The phase cycle is as follows: $\phi_1 = x,-x$; $\phi_2 = x$; $\phi_3 = 2(x),2(y),2(-x),2(-y)$; $\phi_4 = x$; rec. = $x,-x,-x,x$. Quadrature detection in F_1 is achieved with a gradient enhanced sensitivity scheme^{21,22} by recording a pair of data sets with (ϕ_4, G_9) and $(-\phi_4, -G_9)$ for each t_1 point. For each successive t_1 value ϕ_2 is inverted.²³ (b) Multiplet structure obtained in a ^{13}C 90° -acquire experiment involving a $^{13}\text{CD}_2$ spin system; (c) Evolution of the ^{13}C pentet due to ^{13}C - ^2H J_{CD} coupling for a period of $2T_C = 1/(3J_{\text{CD}})$. (d) Components of the magnetization that are along z after the 90°_x ^{13}C pulse at point b in (a) that make up the mode M_L .

theory and with expectations based on ^2H spin relaxation measurements in $^{13}\text{CH}_2\text{D}$ methyl groups.

Materials and Methods

The $\{\text{U-}[^{12}\text{C},^2\text{H}]; \text{methyl-}^{13}\text{CHD}_2\}$ -labeled sample of MSG (82 kDa) used in this work has been prepared as described previously.^{6,12} The MSG sample was 0.80 mM in protein and was dissolved in 99.9% D_2O containing 25 mM sodium phosphate, pH 7.1 (uncorrected), 20 mM MgCl_2 , 0.05% NaN_3 , 5 mM DTT. All experiments on MSG have been recorded at 37°C on a Varian Inova 600 MHz spectrometer equipped with a cryogenically cooled probe. The pulse sequence in Figure 1a was used with variable relaxation delays T of 0.05, 10, 20, 30, 40, 50, and 60 ms. Relaxation rates were extracted from intensities of correlations in $^{13}\text{C},^1\text{H}$ two-dimensional data sets that are comprised of (80, 576) complex points, corresponding to acquisition times of (53, 64) ms in each of (t_1, t_2) . 128 scans were acquired for each complex t_1 value (64 scans for each of the cosine and sine components) along with a relaxation delay of 2 s so that each spectrum was recorded in 6 h.

A 1.8 mM $\{\text{U-}[^{15}\text{N},^{13}\text{C}]; 50\%-[^2\text{H}]\}$ -labeled sample of the 7.5-kDa protein L,¹³ prepared as described previously,⁵ was dissolved in buffer containing 50 mM Na_3PO_4 , pH 6.0, 0.05% NaN_3 , and 10% $^2\text{H}_2\text{O}$. The pulse scheme in the Supporting Information was used to select for $^{13}\text{CHD}_2$ methyl groups from the complete range of methyl isotopomers that is present in the sample and for measurement of $R_1(M_L; ^{13}\text{CHD}_2)$ values (see below). Experiments on protein L were recorded at 500

MHz using a Varian Inova spectrometer equipped with a room-temperature probe. Experiments were performed at temperatures of 5, 25, and 45°C so that the correlation time describing the overall molecular rotation could be varied between 2 and 10 ns in this system. Values of $T = 0.05, 2, 4, 6, 8, 12,$ and 16 ms were used for protein L at all temperatures. Data sets were recorded with (84, 512) complex points, acquisition times of (28, 64) ms in (t_1, t_2) , 128 scans per complex t_1 point, and a relaxation delay of 2 s, for a net acquisition time of 6.4 h/spectrum.

All spectra were processed with NMRPipe/NMRDraw software,¹⁴ and relaxation decays were subsequently fit to single-exponential functions, Ae^{-RT} , to extract the relaxation rate, R . Average values of $R_1(M_L; ^{13}\text{CHD}_2)$ measured in MSG (protein L at 5; 25; 45°C) are 14.1 ± 3.4 (59.8 ± 6.4 ; 56.5 ± 6.5 ; 52.3 ± 6.2) s^{-1} .

Results and Discussion

Theoretical Underpinnings of the Experiment. In the absence of any concerns regarding either sensitivity or resolution, the simplest approach to obtain the time scale of motion of methyl containing side chains via ^2H relaxation in a $^{13}\text{CHD}_2$ probe would be to measure pure ^2H longitudinal relaxation via an inversion recovery type of experiment.^{15,16} In practice, however, such experiments suffer from very poor sensitivity in any application involving biomolecules. Thus, an alternative

(12) Ollerenshaw, J. E.; Tugarinov, V.; Skrynnikov, N. R.; Kay, L. E. *J. Biomol. NMR* **2005**, *33*, 25–41.

(13) Scalley, M. L.; Yi, Q.; Gu, H.; McCormack, A.; Yates, J. R.; Baker, D. *Biochemistry* **1997**, *36*, 3373–82.

(14) Delaglio, F.; Grzesiek, S.; Vuister, G. W.; Zhu, G.; Pfeifer, J.; Bax, A. *J. Biomol. NMR* **1995**, *6*, 277–293.

(15) Poupko, R.; Vold, R. L.; Vold, R. R. *J. Magn. Reson.* **1979**, *34*, 67–81.

(16) Vold, R. L.; Vold, R. R.; Poupko, R.; Bodenhausen, G. *J. Magn. Reson.* **1980**, *38*, 141–161.

approach must be found involving a magnetization mode that is easy to prepare and that relaxes in a (near) single-exponential manner over a broad range of motional parameters with a relaxation time that is “ T_1 -like”.

In what follows we present a succinct explanation of how such a mode (referred to in what follows as M_L) was chosen as a reporter of dynamics. For sensitivity reasons any experiment must begin with initial methyl proton polarization that is subsequently transferred to ^{13}C so that the individual carbon lines (there are five, see Figure 1) can evolve due to the one-bond ^{13}C – ^2H scalar coupling, J_{CD} . The goal is to choose some evolution delay ($2T_C$ in Figure 1a) so that a mode can be prepared with the properties described above. We begin by considering the pulse scheme of Figure 1a that we will show can be used to measure the decay of such a magnetization state for {U- $^{12}\text{C}, ^2\text{H}$ }; methyl- $^{13}\text{CHD}_2$ }-labeled proteins. The experiment is very similar to a scheme for measuring $R_2(^2\text{H}; ^{13}\text{CHD}_2)$ rates that has been described previously.⁶ The evolution of each of the carbon lines in the methyl $^{13}\text{CD}_2$ spin system due to J_{CD} that occurs during the interval between points *a* and *b* (duration $2T_C$) can be described using equations presented previously (see eq 14 of Muhandiram et al.⁴), with the magnetization of interest after the ^{13}C 90° pulse at point *b* of Figure 1a given by

$$M_L(\theta) = C_z(1 - D_{z,1}^2) \left[\frac{1}{2}(D_{z,2}^2 + D_{z,2}) - \frac{1}{2}(D_{z,2}^2 - D_{z,2}) \right] \sin(\theta) + C_z \left[\frac{1}{2}(D_{z,1}^2 + D_{z,1}) - \frac{1}{2}(D_{z,1}^2 - D_{z,1}) \right] (1 - D_{z,2}^2) \sin(\theta) + \left[\frac{1}{4}C_z(D_{z,1}^2 + D_{z,1})(D_{z,2}^2 + D_{z,2}) - \frac{1}{4}C_z(D_{z,1}^2 - D_{z,1})(D_{z,2}^2 - D_{z,2}) \right] \sin(2\theta) \quad (1)$$

with all other terms destroyed by gradient G4. In eq 1, $\theta = 4\pi J_{\text{CD}}T_C$ and $D_{z,q}$ is the z -magnetization from deuterium spin q . The notation used in eq 1 is particularly convenient because it is immediately apparent from where each of the terms is derived. Noting that for a ^{13}C – ^2H two-spin system the center and outer two ^{13}C multiplet components can be represented as $C_x(1 - D_z^2)$, $1/2C_x(D_z^2 + D_z)$, and $1/2C_x(D_z^2 - D_z)$, corresponding to ^{13}C magnetization coupled to deuterons with magnetic quantum numbers $m_l = 0, 1$, and -1 respectively, it becomes clear that the first two lines of eq 1 reflect the evolution of antiphase ^{13}C magnetization that is coupled to deuterons with quantum numbers $(0, \pm 1)$ (line 1 of eq 1) or $(\pm 1, 0)$ (line 2) during $2T_C$, where the first and second numbers in parentheses correspond to m_l values of the first and second deuterons, respectively. The third line arises from evolution due to coupling with deuterons with magnetic quantum numbers $(\pm 1, \pm 1)$.

Following a lengthy, although straightforward calculation, and including relaxation contributions only from the dominant quadrupolar interactions, it can be shown that

$$\frac{dM_L(\theta)}{dT} = -\left(\frac{3}{40}\right) \left(\frac{2\pi e^2 q Q}{h}\right)^2 [(A_1F_1 + A_2F_2)J^A(\omega_D) + (A_3F_1 + A_4F_2)J^A(2\omega_D) + A_5F_3J^C(\omega_D)] \quad (2)$$

where

$$F_1 = C_z(1 - D_{z,1}^2) \left[\frac{1}{2}(D_{z,2}^2 + D_{z,2}) - \frac{1}{2}(D_{z,2}^2 - D_{z,2}) \right] + C_z \left[\frac{1}{2}(D_{z,1}^2 + D_{z,1}) - \frac{1}{2}(D_{z,1}^2 - D_{z,1}) \right] (1 - D_{z,2}^2) = C_z(1 - D_{z,1}^2)D_{z,2} + C_zD_{z,1}(1 - D_{z,2}^2) \\ F_2 = \frac{1}{4}C_z(D_{z,1}^2 + D_{z,1})(D_{z,2}^2 + D_{z,2}) - \frac{1}{4}C_z(D_{z,1}^2 - D_{z,1})(D_{z,2}^2 - D_{z,2}) = \frac{1}{2}C_z(D_{z,1}^2D_{z,2} + D_{z,1}D_{z,2}^2) \\ F_3 = \frac{1}{4}C_zD_{-1}(D_{z,2}D_{+2} + D_{+2}D_{z,2}) + \frac{1}{4}C_zD_{+1}(D_{z,2}D_{-2} + D_{-2}D_{z,2}) + \frac{1}{4}C_z(D_{z,1}D_{+1} + D_{+1}D_{z,1})D_{-2} + \frac{1}{4}C_z(D_{z,1}D_{-1} + D_{-1}D_{z,1})D_{+2} \quad (3)$$

and

$$A_1 = 3 \sin(\theta) - \sin(2\theta) \\ A_2 = -2 \sin(\theta) + 2 \sin(2\theta) \\ A_3 = 4 \sin(\theta) \\ A_4 = 4 \sin(2\theta) \\ A_5 = 2 \sin(\theta) - \sin(2\theta) \quad (4)$$

In eqs 2,3

$$J(\omega) = \frac{1}{9} S_{\text{axis}}^2 \frac{\tau_C}{1 + (\omega\tau_C)^2} + \left(P_2(\cos \alpha) - \frac{1}{9} S_{\text{axis}}^2 \right) \frac{\tau_e}{1 + (\omega\tau_e)^2} \quad (5)$$

and $D_{\pm} = D_x \pm iD_y$; $e^2qQ/h = 167$ kHz is the ^2H quadrupolar coupling constant;¹⁷ S_{axis} is the generalized order parameter of the methyl three-fold axis; $P_2(x) = (1/2)(3x^2 - 1)$, $\alpha = 0^\circ$, and $P_2(\cos \alpha) = 1$ for the autocorrelation spectral density, $J^A(\omega)$, while $\alpha = 109.5^\circ$ and $P_2(\cos \alpha) = -1/3$ for the cross-correlation spectral density, $J^C(\omega)$; τ_C is the rotational correlation time of the assumed isotropic global molecular reorientation, and $1/\tau_e = 1/\tau_f + 1/\tau_C$, where τ_f is the correlation time of (fast) local motions.

We require that $M_L(\theta)$ decays exponentially in the limit that only autospectral density terms are taken into account. From eq 2 it follows, therefore, that

$$A_1F_1 + A_2F_2 \propto A_3F_1 + A_4F_2 \quad (6)$$

and thus,

$$\frac{A_1}{A_2} = \frac{A_3}{A_4} \quad (7)$$

from which we obtain $\theta = (2/3)\pi$. Inserting this value of θ into eq 2 gives

$$\frac{d(M_L)}{dT} = -\left(\frac{3}{40}\right)\left(\frac{2\pi e^2 q Q}{h}\right)^2 \{4J^A(\omega_D) + 4J^A(2\omega_D)\}M_L + 3J^C(\omega_D)F_3 \quad (8)$$

where $M_L = F_1 - F_2 = C_z(D_{z,1} + D_{z,2}) - \frac{3}{2}C_z(D_{z,1}D_{z,2}^2 + D_{z,1}^2D_{z,2})$. A similar equation exists for the relaxation of F_3 ,

$$\frac{dF_3}{dT} = -\left(\frac{3}{40}\right)\left(\frac{2\pi e^2 q Q}{h}\right)^2 \{2J^C(\omega_D)M_L + [3J^A(0) - 3J^C(0) + 3J^A(\omega_D) + 2J^A(2\omega_D) + 2J^C(2\omega_D)]F_3\} \quad (9)$$

Equations 8 and 9 can be re-expressed in the following matrix representation

$$\frac{d}{dT} \begin{bmatrix} M_L \\ F_3 \end{bmatrix} = - \begin{bmatrix} R_1(M_L) & \sigma_{12} \\ \sigma_{21} & R_1(F_3) \end{bmatrix} \begin{bmatrix} M_L \\ F_3 \end{bmatrix} \quad (10.1)$$

where

$$\begin{aligned} R_1(M_L) &= \left(\frac{3}{40}\right)(2\pi e^2 q Q/h)^2 \{4J^A(\omega_D) + 4J^A(2\omega_D)\} \\ R_1(F_3) &= \left(\frac{3}{40}\right)(2\pi e^2 q Q/h)^2 \{3[J^A(0) - J^C(0)] + 3J^A(\omega_D) + 2[J^A(2\omega_D) + J^C(2\omega_D)]\} \\ \sigma_{12} &= \left(\frac{3}{40}\right)(2\pi e^2 q Q/h)^2 \{3J^C(\omega_D)\} \\ \sigma_{21} &= \left(\frac{3}{40}\right)(2\pi e^2 q Q/h)^2 \{2J^C(\omega_D)\} \end{aligned} \quad (10.2)$$

The solution of the system of differential eqs 10.1–10.2 for the time dependence of M_L with initial conditions that are appropriate to the experiment of Figure 1a, $M_L(0) = 1$ and $F_3(0) = 0$, is given by

$$\begin{aligned} M_L(T) &= \frac{1}{2} \frac{\{R_1(M_L) - R_1(F_3) + \sqrt{\epsilon}\}}{\sqrt{\epsilon}} \times \\ &\quad \exp\left\{-\frac{1}{2}[R_1(M_L) + R_1(F_3) + \sqrt{\epsilon}]T\right\} - \\ &\quad \frac{1}{2} \frac{\{R_1(M_L) - R_1(F_3) - \sqrt{\epsilon}\}}{\sqrt{\epsilon}} \times \\ &\quad \exp\left\{-\frac{1}{2}[R_1(M_L) + R_1(F_3) - \sqrt{\epsilon}]T\right\} \end{aligned} \quad (11.1)$$

where

$$\epsilon = [R_1(M_L) - R_1(F_3)]^2 + 4\sigma_{12}\sigma_{21} \quad (11.2)$$

Although from eqs 8–11 it is clear that the relaxation of M_L is not purely single-exponential, simulations that we have performed for (S_{axis}^2 , τ_f , τ_c) values within (0.1–0.9, 2–100 ps, 2–60 ns) and for relaxation delays extending to $1/R_1(M_L)$ show that the relaxation of M_L is very well approximated by the expression for $R_1(M_L)$ given above. The simulations show further that the errors in the extracted rates, assuming single-exponential relaxation, are less than ~ 2 –3% for the most commonly obtained values of dynamics parameters in methyl groups of proteins (see Supporting Information). Finally, it is worth noting that contributions to R_1 from dipolar interactions are very much smaller than those from the quadrupolar terms considered above and can be safely ignored.¹⁸

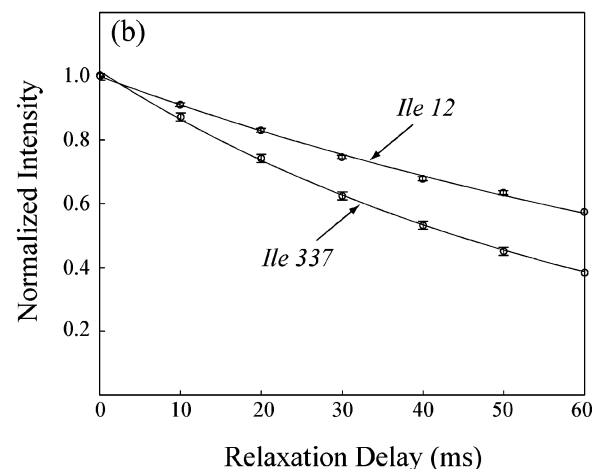
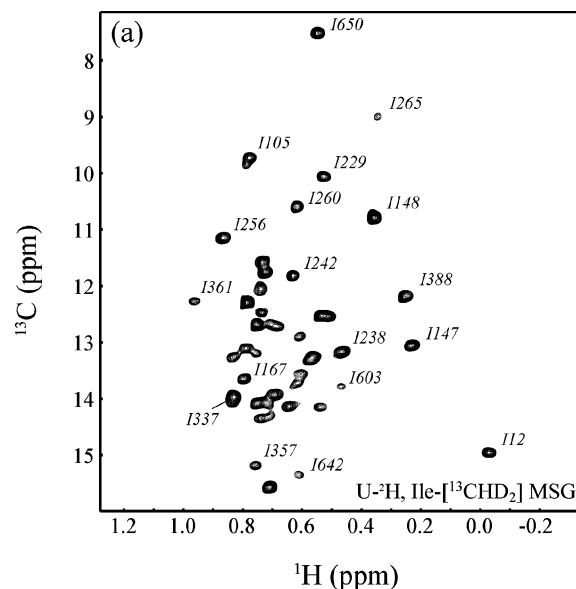


Figure 2. (a) $^{13}\text{C}, ^1\text{H}$ correlation map of {U- $^{12}\text{C}, ^2\text{H}$ }; methyl- $^{13}\text{CHD}_2$ }-labeled MSG, 37 °C, 600 MHz, recorded with the scheme of Figure 1a, $T = 0.05$ ms. (b) Decay curves for residues Ile 12 and Ile 337, along with fits to a single-exponential decay function (solid lines).

The results of the preceding discussion can be presented “visually” (Figure 1b–d). By choosing an evolution delay of $2T_C = 1/(3J_{\text{CD}})$ (between points *a* and *b* in Figure 1a) each component of what would be a pentet structure in a ^{13}C 90° pulse-observe experiment (Figure 1b) acquires the phase illustrated in Figure 1c. The ^{13}C 90° pulse at point *b* of Figure 1a projects the *y*-magnetization components along the *z*-axis, Figure 1d, and the subsequent gradient G4 destroys all other coherences. This creates the desired mode, $M_L = C_z\{D_{z,1} + D_{z,2} - \frac{3}{2}(D_{z,1}D_{z,2}^2 + D_{z,1}^2D_{z,2})\}$, whose decay rate (referred to as $R_1(M_L; ^{13}\text{CHD}_2)$) is subsequently measured as a function of the variable delay T (Figure 1a).

Prior to the transfer of magnetization back to ^1H for detection, ^{13}C chemical shift is recorded, as illustrated in Figure 1a, so that a series of ^{13}C – ^1H correlation maps are generated with the intensity of correlations evolving as $\exp(-R_1(M_L; ^{13}\text{CHD}_2)T)$. Because the evolution period $2T_C$ is double that used for the measurement of $R_2(^2\text{H}, ^{13}\text{CHD}_2)$,⁶ the sensitivity of data sets

(18) Yang, D.; Kay, L. E. *J. Magn. Reson., Ser. B* **1996**, *110*, 213–218.

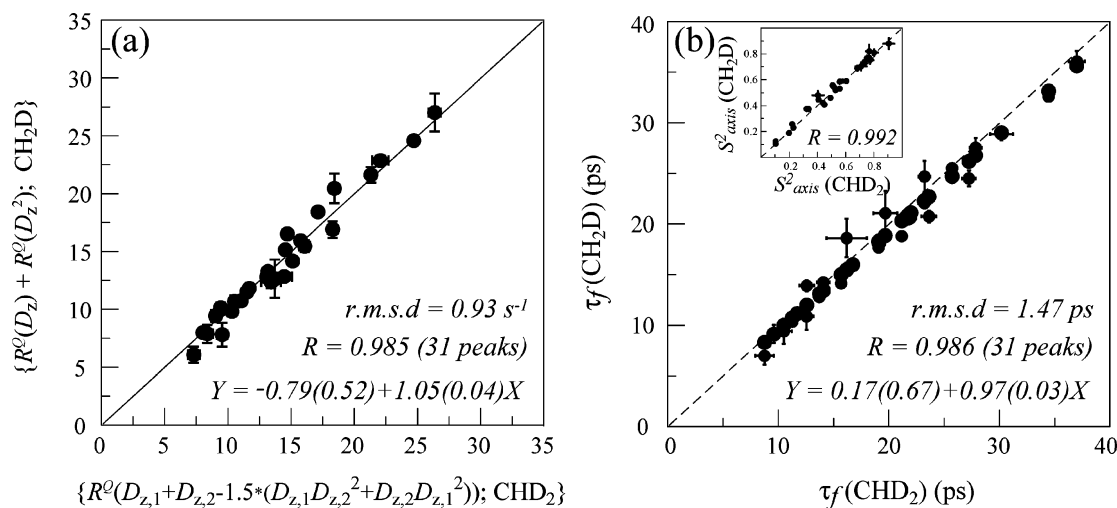


Figure 3. Linear correlation plots of (a) $R_1(M_L; {}^{13}CHD_2)$ (x-axis) vs $\{R^Q(D_z) + R^Q(D_z^2); {}^{13}CH_2D\}$ (y-axis), measured for Ile δ 1-methyls of MSG (600 MHz, 37 °C); all rates are in s^{-1} ; (b) ${}^{13}CHD_2$ -derived τ_f (x-axis) vs ${}^{13}CH_2D$ -derived τ_f values⁶ (y-axis). Rotational correlation times of 54 and 56 ns have been used in the analysis, as described previously.⁶ Linear regression parameters are shown for each plot in panels a,b along with Pearson's correlation coefficient, R , and pairwise rmsd values between the two sets of data.

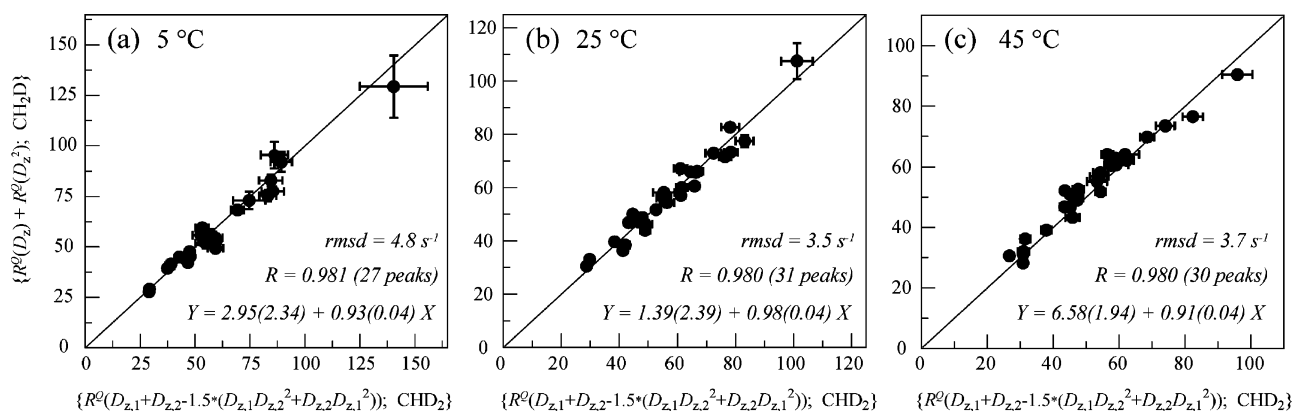


Figure 4. Linear correlation plots of $R_1({}^{13}CHD_2)$ (x-axis) vs $\{R^Q(D_z) + R^Q(D_z^2); {}^{13}CH_2D\}$ (y-axis), measured in methyl groups of $\{U-[{}^{15}N, {}^{13}C]; \sim 50\%-[{}^2H]\}$ -labeled protein L (500 MHz) at 5, 25, and 45 °C; all rates are in s^{-1} . Linear regression parameters are shown for each plot in panels a–c along with Pearson's correlation coefficient, R , and pairwise rmsd values between the two sets of data.

recorded with the present scheme is approximately 2–2.5-fold lower than that of spectra that measure R_2 in the case of MSG.

Experimental Verification. Figure 2a shows a ${}^{13}C, {}^1H$ correlation map of $\{U-[{}^{12}C, {}^2H]; \text{methyl-}{}^{13}CHD_2\}$ -labeled MSG, 37 °C, recorded with the scheme of Figure 1a, $T = 0.05$ ms. Figure 2b shows decay curves for residues Ile 12 and Ile 337, as well as fits (solid lines) of the decays to single-exponential functions, from which $R_1(M_L; {}^{13}CHD_2)$ is obtained.

It can be shown that $R_1(M_L; {}^{13}CHD_2) = R^Q(D_z; {}^{13}CH_2D) + R^Q(D_z^2; {}^{13}CH_2D)$, where the R^Q rates are those associated with the relaxation of the density elements D_z and D_z^2 that are commonly measured in experiments focusing on ${}^{13}CH_2D$ methyl isotopomers, as described previously.⁵ Thus, a correlation plot of experimental $R_1(M_L; {}^{13}CHD_2)$ vs $R^Q(D_z; {}^{13}CH_2D) + R^Q(D_z^2; {}^{13}CH_2D)$ rates can be used to validate the methodology. Figure 3a illustrates the level of agreement obtained in studies of Ile δ 1-methyls from MSG. Figure 3b shows τ_f values obtained from combined analysis of $R_1(M_L; {}^{13}CHD_2)$ and $R_2({}^2H, {}^{13}CHD_2)$ relaxation rates of Ile δ 1 groups in Ile δ 1- $[{}^{13}CHD_2]$ MSG or via fits of $R^Q(D_{+})$ and $R^Q(D_{-})$ rates measured earlier in an Ile δ 1-

$[{}^{13}CH_2D]$ -labeled sample.⁶ A comparison of S^2_{axis} values obtained from the same data sets is also presented in the inset to the figure.

Figure 4 shows similar levels of agreement generated from measurements involving protein L that have been performed at a number of temperatures where the correlation time of the protein ranges from 2 (45 °C) to 10 (5 °C) ns. Taken together the experimental data presented provide strong evidence that the new experimental measure of the time scale of methyl containing side-chain dynamics is robust. This is consistent with simulations that show that despite the fact that differential relaxation of outer and inner lines of the ${}^{13}C$ - 2H pentet in Figure 1b can occur¹⁹ during the period $2T_C$ (Figure 1a), the deviations

- (19) Werbelow, L. G.; Morris, G. A.; Kumar, P.; Kowalewski, J. *J. Magn. Reson.* **1999**, *140*, 1–8.
- (20) Shaka, A. J.; Keeler, J.; Frenkiel, T.; Freeman, R. *J. Magn. Reson.* **1983**, *52*, 335–338.
- (21) Kay, L. E.; Keifer, P.; Saarinen, T. *J. Am. Chem. Soc.* **1992**, *114*, 10663–10665.
- (22) Schleucher, J.; Sattler, M.; Griesinger, C. *Angew. Chem., Int. Ed. Engl.* **1993**, *32*, 1489–1491.
- (23) Marion, D.; Ikura, M.; Tschudin, R.; Bax, A. *J. Magn. Reson.* **1989**, *85*, 393–399.

from the expected intensities are small and do not introduce significant artifacts in the data, at least for proteins with the range of correlation times examined here (2 to 54 ns).

In summary, we have presented an approach in which multiplet lines are combined in such a way as to generate a magnetization mode having certain desired properties. In the present case a pulse scheme has been derived that selects a ^2H -magnetization mode in $^{13}\text{CHD}_2$ methyl groups that relaxes in a T_1 -like manner, from which the time scale of local methyl dynamics can be obtained. A combined analysis of ^2H $R_1(M_L)$ and R_2 rates from $^{13}\text{CHD}_2$ methyl probes is now possible so that $(S_{\text{axis}}^2, \tau_f)$ parameters can be obtained exclusively from these values.

Acknowledgment. This work was supported by a Canadian Institutes of Health Research (CIHR) grant to L.E.K. and a

CIHR postdoctoral fellowship to V.T. L.E.K. holds a Canada Research Chair in Biochemistry. V.T. dedicates this paper to the memory of his father who passed away on July 14 in Moscow, Russia.

Supporting Information Available: Figures are provided showing the pulse scheme developed for $R_1(M_L; ^{13}\text{CHD}_2)$ measurements in U- ^{13}C -labeled and partially deuterated proteins, as well as contour plots showing $R_1(M_L; ^{13}\text{CHD}_2)$ and simulated errors in $R_1(M_L; ^{13}\text{CHD}_2)$ that can arise from cross-relaxation of M_L and F_3 as a function of $(S_{\text{axis}}^2, \tau_f, \tau_C)$. This material is available free of charge via the Internet at <http://pubs.acs.org>.

JA063071S